INSTITUTE OF PHYSICS PUBLISHING JOURNAL OF PHYSICS: CONDENSED MATTER

J. Phys.: Condens. Matter **14** (2002) 7449–7459 PII: S0953-8984(02)37931-1

Densification of silica glass under pressure

Kostya Trachenko[1,2] **and Martin T Dove**[1]

[1] Department of Earth Sciences, University of Cambridge, Downing Street, Cambridge CB2 3EQ, UK
[2] Cavendish Laboratories, University of Cambridge, Madingley Road, Cambridge CB3 0HE, UK

E-mail: kot@esc.cam.ac.uk

Received 11 June 2002
Published 2 August 2002
Online at stacks.iop.org/JPhysCM/14/7449

Abstract

We present the results of a simulation study of the effects of pressure on structural changes in silica glass. We observe structural relaxations in glass under pressure that involve large atomic displacements and are accompanied by breaking of the original bonds and forming of new ones. A large proportion of the new topological arrangements formed during pressurizing are preserved in structures on decompression, resulting in the irreversibility of topological changes. Substantial rebonding makes the mechanism of densification in glass essentially different from that present in transitions between crystalline silicas. We find that higher temperature promotes the degree of rebonding and densification in decompressed structure.

1. Introduction

Silica glass has attracted a lot of research in view of its geological and technological importance, in addition to the fact that it has become a prototype model of a continuous random network in amorphous materials. Pressure-induced phenomena in silica glass have been studied intensively using various experimental techniques [1, 2]. When compressed beyond 25 GPa, silica glass becomes irreversible on decompression, showing about 20% increase in density [1, 2]. Molecular dynamics simulations have been important in the understanding of the structure of glass at elevated pressures, as well as the decompressed structures [2–4]. It has been shown that the densification of silica glass is accompanied by an increase in the average coordination number [3, 4], and the densification on decompression has been correlated with this increase in coordination numbers [4]. However, the microscopic details and mechanism of the densification process are not yet fully understood. Pressurizing the crystalline form of silica with fourfold-coordinated silicon atoms to stishovite with sixfold-coordinated atoms is obviously accompanied by the appearance of two new Si–O bonds per Si atom, and the newly formed bonding remains metastable when the pressure is released. In this paper we show that

densification in silica glass involves another important mechanism that involves substantial changes in local topology and rebonding.

We use molecular dynamics simulation methods to explore the effect of pressure on the structure of silica glass, considering a wide range of pressures. We start with the effect that pressures up to ∼3 GPa have on the double-well potentials (DWP), namely those that we recently identified and studied in silica glass [5–7] in the context of the model of two-level tunnelling states [8]. At zero pressure, large atomic jump motions in DWP occur in certain 'active' regions of the structure. We find in this paper that small increases of pressure change the location of 'active' regions. DWP appear to be distributed uniformly in glass structure, but some have too large barriers for jumps to be seen and become 'active' when pressure is applied.

Extending the study to higher pressures, we find that as pressure increases and causes an increase of the average coordination numbers, patches of the glass structure become locally unstable, with atomic relaxations occurring in the form of large-amplitude atomic displacements. These involve breaking of original bonds and forming of new bonds, and it is possible to observe the transfer of higher coordination number between SiO_x polyhedra. On decompression, the glass configuration retains the newly formed atomic arrangements, resulting in the irreversibility of topological changes. We quantify the degree of rebonding and show that it is a considerable effect. Rebonding processes observed in this work provide the microscopic mechanism for the continuous relaxation observed experimentally in the pressurized silica glass [9].

Finally, previous simulation work has addressed changes in the silica glass structure under pressure at a given temperature [2–4]. In this paper we study the effects of higher temperature on the structure of compressed and decompressed samples. We find that higher temperature promotes rebonding and densification of decompressed samples.

2. Simulation details

The work reported here was performed using molecular dynamics simulations. We used the code DL_POLY [10], which has been optimized for use on parallel computers. The starting atomic configurations of silica glass were obtained from the configurations of amorphous silicon formed by the Wooten–Weaire algorithm [11]. Oxygen atoms were inserted along each Si–Si bond, and the structures were then relaxed in the simulations. We showed previously [6] that the radial distribution functions (RDF) of the relaxed structures and the calculated neutron scattering function are in excellent agreement with experimental data. Most of our simulations were performed using a configuration containing 4096 SiO_4 tetrahedra with periodic boundary conditions.

We used the interatomic potential of Tsuneyuki *et al* [12]. This model uses standard potential functions which have been parametrized using quantum mechanical calculations on small clusters. It has been shown that the model is able to reproduce high-pressure silica polymorphs, as well as phase transitions at external pressure [12, 13]. This potential has been recently used in the simulation studies to address pressure effects in silica glass (see, for example, [4, 14, 15]), and is believed to adequately handle increased coordinations (see [4] and references therein).

In the molecular dynamics simulations, we performed the simulations aimed at achieving equilibration during compression and decompression in stages using constant-pressure/temperature (NPT) ensembles. Structures were equilibrated at a given pressure for 20 ps. To then study the evolution of structures at a given pressure, we performed simulations in constant-volume/energy (NVE) ensembles. The pressure effects have been

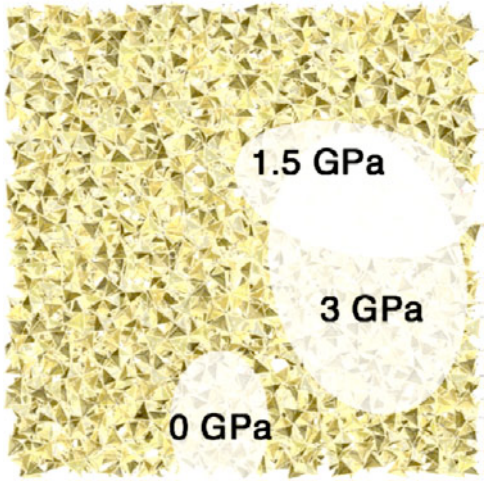

Figure 1. Regions of glass structure that, at different pressures, become 'active' in the sense of being able to support atomic motions in DWP. These active regions are denoted by the ellipses, which in the projection are slightly overlapping for two pressures.

(This figure is in colour only in the electronic version)

simulated at different temperatures, and the structures have been equilibrated at their respective temperatures before applying pressure.

3. Results and discussion

3.1. The effect of pressure up to 3 GPa on DWP

Before embarking on discussion about the irreversible structural changes under pressure, we note that previously we have found that silica glass supports floppy modes, as well as large-amplitude tetrahedral reorientations that occur in DWP [5–7]. Effects of pressure on floppy modes have been reported recently [16], and below we study how pressure changes the distribution of DWP in glass structure. DWP were found to exist in some 'active regions', and we proposed that the atomic motions in these DWP are responsible for the existence of two-level tunnelling states [8] that give rise to anomalous thermal properties of glasses at low temperatures [17]. We have seen that the motions in DWP involve large-amplitude cooperative reorientations of several tens of SiO_4 tetrahedra [5, 6]. It is interesting to see how these DWP react to external pressure. In this paper we are concerned with pressures up to 3 GPa which, as will be discussed later, preserve the tetrahedral topology of glass.

The structures equilibrated at low temperature $T = 50$ K, were pressurized in stages up to $P = 3$ GPa. In the constant-energy simulations of structures at various pressures we have calculated distribution functions of the squared values of atomic displacements, and used these to identify atoms that experienced unusually large jumps, typically around 1 Å. The family of locations of these atoms form the 'active' regions in glass structure [5, 6]. We find that even small changes in pressure of $\sim$0.1 GPa result in the disappearance of atomic jumps in the regions that have been 'active' at a different pressure (including zero pressure). Instead, atomic jumps arise in new 'active' regions of the structure; figure 1 illustrates this point.

It appears that DWP are distributed evenly in the glass structure, but some have inaccessibly high barriers for reorientations to occur at a given simulation temperature. Changing pressure

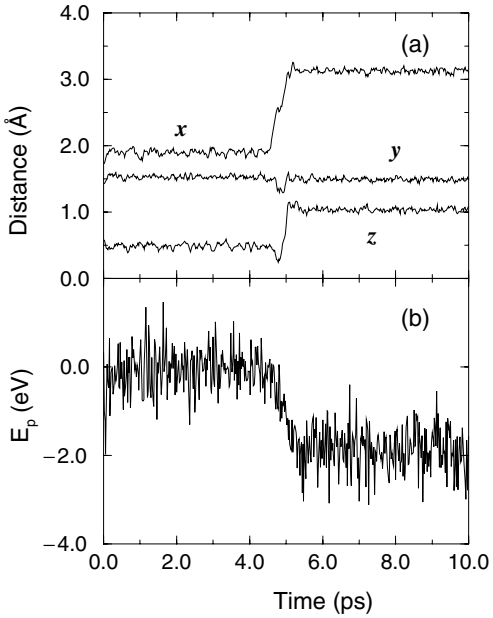

Figure 2. Time dependence of atomic coordinates x, y, z (in orthogonal Å units) for the O atom undergoing a large jump involving a movement of about 1.5 Å (a), and the time dependence of the potential energy of the system (with a constant value subtracted) through the jump event (b).

lowers the heights of some DWP barriers and increases them for the others. This is the new insight into how DWP are distributed in glass, and is consistent with the isotropic nature of atomic arrangements in glass structure. Note that the motion in DWP at low pressures occurs within the tetrahedral network and the structures are reversible on decompression.

3.2. Rebonding events at elevated pressures

We now address the irreversible changes that occur in the structures of silica glass at elevated pressures in the range 3–40 GPa at low temperature $T = 50$ K. We use the same distribution-function procedure for identifying the atoms in the structure that experience large jumps as described in the previous section. In figure 2(a) we show the trajectory of an atom that experienced a jump of $\sim$1.5 Å in the NVE simulation at 20 GPa. Figure 2(b) shows that the corresponding change in the potential energy of the configuration in this jump event is $\sim$2 eV. Such a change in energy is much larger that the one we observed in the DWP at zero pressure [5, 6] and, together with large magnitude of the atomic jump, this has prompted us to study the local environment of that atom before and after the jump. Figures 3(a) and (b) show the structures in the vicinity of the atom that experienced the jump shown in figure 2. In this event, the O atom that is shared by two Si atoms across the ring of SiO_n polyhedra (marked by two arrows in figure 3(a)) changes the bonding to two different Si atoms in the ring. At the same time, other closely located O atoms (marked by arrows in figure 3(a)) participate in the rebonding. This process can be described as an event in which the coordination number of one Si atom is transferred to a neighbouring Si atom. Because of the specific nature of this event, and particularly since it is not involved in the initial densification process, we have called it a 'coordinon'. The coordinon represents the ability of the structure to rearrange the bonds dynamically at constant volume *after* the application of pressure has caused the initial atomic

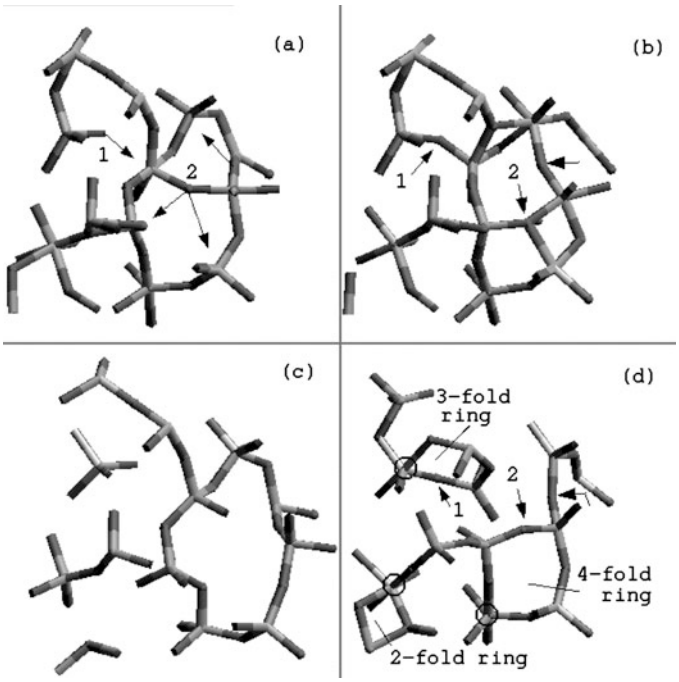

Figure 3. Local structures of silica glass at 50 K showing (a) a small atomic configuration within the simulation after compression to 20 GPa but before the coordinon relaxation; (b) the same atomic configuration at 20 GPa after a coordinon relaxation takes place; (c) the same configuration in (a) after being decompressed from 20 GPa without the coordinon relaxation having taken place; and (d) the configuration of the structure decompressed from 20 GPa after the coordinon relaxation of (b) has taken place. Si and O atoms are drawn light and dark, respectively. Arrows in (a) point from atoms that experience large jumps and rebonding during the coordinon relaxation at 20 GPa, and towards the final positions in which they form new bonds. Arrows in (b) point towards the final positions of the atoms that have jumped in (a). The atoms are indicated by the arrows in (d). The circles in (d) show Si atoms with increased coordination. The animation showing the rebonding event is available in the electronic form of the journal and can also be downloaded from http://www.esc.cam.ac.uk/movies.

rearrangement and densification. We will see below that it is the existence of coordinons that primarily leads to irreversibility in the pressure-induced changes of the glass structure, not merely the initial pressure-induced rebonding events themselves. After a coordinon event, the configuration with the newly formed bonding can be stable in the simulations for several tens of picoseconds, a point to which we return later. The animation showing the rebonding event is available in the electronic form of the journal and can also be downloaded from http://www.esc.cam.ac.uk/movies.

On decompression, the atoms in the vicinity of the coordinon preserve the newly formed bonding. To demonstrate this, we have decompressed the structure from 20 GPa before and after the rebonding has occurred, and plotted the structures in figures 3(c) and (d) respectively. By comparing the atomic arrangements in figures 3(c) and (d) we see that the coordinon relaxation results in different topological arrangements of atoms in the decompressed structures. Furthermore, by comparing the decompressed structure with the initial uncompressed structure, which is not shown in figure 3, we find that the arrangement of atoms in the decompressed structure before the coordinon relaxation takes place (figure 3(c))

is close to the arrangement and topology in the initial structure. On the other hand, the 'memory' of the arrangement of atoms in the initial structure is essentially lost in the structure decompressed from 20 GPa after the coordinon relaxation takes place (figure 3(d)).

It follows from figure 3 that it is the coordinon relaxation that gives rise to the appearance of defects in the decompressed structure. These include increased local coordination numbers and small rings of SiO_x polyhedra [3, 4]. By comparing figures 3(a) and (b) it can be seen that the structure under pressure relaxes to the topology that is favoured by that pressure, and that contains defects such as Si atoms with increased fivefold and sixfold coordinations and Si rings with the number of members reduced to 2–4 (see figure 3(b)). For example, the fourfold ring in the decompressed structure (figure 3(d)) is created by the jump of atom 2, changing the number of Si atoms in the ring from fivefold to fourfold and subsequent elimination of energetically unfavourable twofold ring on decompression, as shown in the rebonding event in figures 3(a), (b). Similarly, the threefold ring in the decompressed structure (figure 3(d)) appears as atom 1 acquires the new bond in the same rebonding event, closing the fourfold ring as shown in figure 3(b), which transforms into the threefold ring on decompression. On the other hand, no high-pressure defects are seen in the structure that has been decompressed *before* the coordinon relaxation takes place (see figure 3(c)). It appears that in addition to causing the irreversible changes in topology of structure on decompression, the coordinon events have the function of carrying the elements of the high-pressure structure into the decompressed structure. We have analysed structures compressed to several pressures in the range between 3 and 40 GPa, and have seen similar rebonding events, all resulting in the same effects as were discussed above.

An analogy with Rubik's cube may be appropriate. A single twist of the cube leads to a state that can easily be transformed back to the original state. On the other hand, a second twist leads to a state that is much harder to transform back to the original state. In silica glass, the first changes in structure on pressurization can be easily reversed on decompression (as in figure 3(a)), and these correspond to the first twist of Rubik's cube. The coordinon event (as in figure 3(b)) then acts as the second twist of Rubik's cube, and makes it much harder for the structure to revert back to its original state on decompression, particularly since there is no longer any driving force for this. Thus the coordinon directly leads to the retention of defects on decompression.

Note that the rebonding events such as the coordinon event shown in figure 3 could be viewed as a motion in some DWP. The difference from the motion in DWP at low pressure discussed in the previous section is that the jump event in figure 3 involves an irreversible change of the local topology and the landscape of the local configurational energy.

It should be noted that we find regions in the structure where no rebonding events take place and yet locally the decompressed structure does not return to its initial topology. This occurs when additional Si–O bonds, formed under pressure, stay intact on decompression, without breaking old bonds. Higher temperature appears to promote rebonding in these regions. We have performed NVE simulations at elevated temperatures $T = 300$, 600, 900 and 1200 K, with prior equilibration at an elevated temperature in the NPT ensemble. We observe that at higher T, rebonding events occur in the parts of glass structure where no rebonding is seen at low T. This point will be revisited below.

3.3. Degree of rebonding and densification process

It is important to quantify the number of rebonding events on compression and decompression and hence to estimate the role of rebonding in irreversible densification. We set up the list of neighbour O atoms to which a Si atom is bonded at each pressure, both on compression and decompression. This allows us to directly compare two structures, which we denote as A and B,

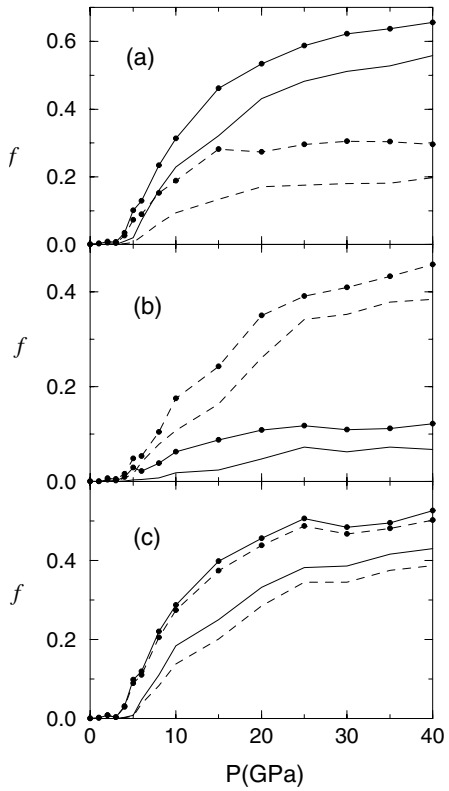

Figure 4. Rebonding efficiency f as a function of pressure P, calculated by comparing (a) the initial uncompressed structure with the structure at elevated P, (b) the structure at elevated pressure P and the structure decompressed from pressure P and (c) the initial uncompressed structure with the structure decompressed from pressure P. Solid curves and dashed curves show new and broken bonds, respectively, at 50 K. Circled solid curves and circled dashed curves show new and broken bonds, respectively, at 1200 K.

at different pressures in terms of the number of broken and new bonds. If an O atom from the neighbour list of a given Si atom from structure A is not on the list of the corresponding Si atom in structure B, then one Si–O bond is counted as broken. Similarly, if an O atom from the neighbour list of a given Si atom from structure B is not on the corresponding Si list in structure A, then one Si–O bond is counted as new.

On compression, we compare the initial structure at zero pressure (structure A) with the structure at elevated pressure P (structure B) and calculate the number of new and broken bonds as described above. We introduce the rebonding efficiency f, which is the ratio of the number of new bonds to the total number of bonds in the initial structure at zero pressure (the latter being equal to four times the number of Si atoms in the structure). This means that at a given pressure, the average number of Si–O bonds for each Si atom changes by $4f$. In fact we can define f separately for newly formed bonds and for broken bonds, and we plot both types of f as functions of P in figure 4(a). On decompression, we can compare the structure at pressure P (structure A) with the structure decompressed from that pressure (structure B), and we plot f for new and broken bonds in figure 4(b). Finally, we can compare the initial structure at zero pressure and the structure decompressed from pressure P and plot both types of f as functions of P in figure 4(c).

There are several points to make about the dynamics of the new and broken bonds from figure 4. The structure is compressible without the need to break old or form new bonds up to $P \sim 3$ GPa. After $P \sim 3$ GPa, new bonds start to form, with f for the formation of new bonds reaching about 55% at $P = 40$ GPa at low temperature (see figure 4(a)). Together with the formation of new bonds, old bonds get broken, often through coordinon events, with f for broken bonds reaching 20% at $P = 40$ GPa at low temperature.

On decompression, the rebonding is dominated by breaking bonds in the compressed structure over the formation of new ones (see figure 4(b)). These include the bonds originally present, and the bonds formed during compression. The important point is that the major proportion of new bonds formed during compression do not break on decompression, and the major proportion of bonds broken on compression do not reinstate themselves on decompression. Figure 4(c) demonstrates this point: the net effect of compression and decompression is that a large proportion of the bonds in the decompressed structure are newly formed. At the same time, a large proportion of bonds present in the original uncompressed structure are broken in the decompressed structure. The values of f, for both new and broken bonds, reaches $\sim$40% at high pressure when the sample is held at low temperature (see figure 4(c)). This is a large effect and highlights the importance of rebonding in the mechanism of irreversible densification in glass.

We can now compare the mechanisms of densification of amorphous and crystalline silica. As we noted in the previous section, there are regions in the glass structure that densify without the breaking of old bonds, with the number of such regions decreasing as temperature increases (see also below). This mechanism of densification is similar to that in the phase transition between low-pressure crystalline silica and stishovite. When stishovite is formed, f changes by 50% at the phase transition, as two new Si–O bonds are formed per Si atom. This is accompanied by the increase of density over coesite [12]. The densified structure is stable at zero pressure, and no bonds break on removal of the pressure.

In silica glass, such a densification mechanism may be supported in some local regions of the structure, but the overall bonding in the decompressed structure is the result of each Si atom acquiring on average $4f$ new Si–O bonds, *and losing* $4f$ bonds that are present in the original structure, with f reaching 40% at $P = 40$ GPa at low temperature. Unlike in crystalline silica, compression and decompression of the topologically disordered glass structure are necessarily accompanied by continuous rebonding. On decompression, $\sim$20% of densification remains due to the stability of the bonding that has been formed under pressure.

We note that experimentally, the volume of compressed glass structure increases logarithmically with time [9], providing evidence for the continuous relaxation processes in pressurized glass. Evolving the pressurized glass samples in the molecular dynamics simulation, we also observe volume decrease. Volume decrease is accompanied by continuous rebonding, during which a surplus of newly formed bonds is formed over the broken ones, leading to the transition towards more closely packed structure. The structure appears to be constantly adjusting to elevated pressure by local processes of rebonding that lead to densification.

Although simulation times are limited (the longest annealing time in this simulation was about 1 ns), inhibiting the quantitative comparison with the experiment, the correlation between volume decrease and rebonding processes is clear. We therefore suggest that rebonding processes described in this work are responsible for the relaxation processes observed experimentally [9]. The quantitative results of the simulation of annealing for longer times will be reported separately.

The fact that pressurized silica glass is not in equilibrium on either compression or decompression, as witnessed by continuous relaxation processes, is important in deciding whether the densification in silica glass can be viewed as a first-order phase transition; the issue

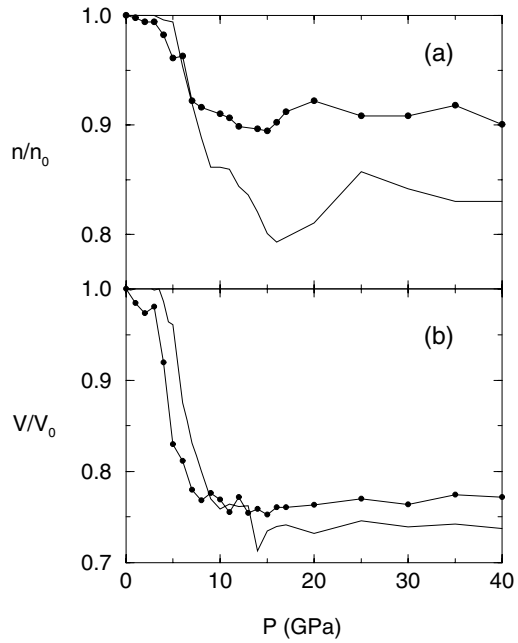

Figure 5. Fraction of fourfold-coordinated Si atoms (a) and relative volume of decompressed samples (b) as a function of applied pressure. Solid and circled solid curves show simulation at 50 and 1200 K, respectively. V_0 is the initial volume of uncompressed structures at each temperature.

that has been recently debated [15, 18]. This will be discussed separately in detail, but here we note that the results of this simulation support the picture of the continuous transformation [9], rather than the first-order phase transition.

3.4. Temperature effects

Higher temperature increases the number of new and broken bonds on compression and decompression, as follows from figures 4(a), (b). This is consistent with the increased number of rebonding events seen at elevated temperature, as mentioned in the previous section.

To explore the effect of temperature on the structures of the decompressed samples, we have calculated the relative numbers of fourfold-coordinated Si atoms in the decompressed structures and relative volume change as a function of pressure P at two different temperatures, as plotted in figure 5(a). We observe that for pressures smaller than $\sim$10 GPa, higher temperature results in the higher degree of densification in the decompressed structures. This is consistent with recent *in situ* measurements [19]. Temperature induced densification will be discussed in more detail separately, but we note here that in our picture this effect has its origin in the higher temperature inducing more rebonding events in the structure, which increases the irreversible changes in topology that are responsible for the densification in the decompressed structures.

4. Summary

To conclude, we have addressed the effects of pressure up to 3 GPa on the DWP in silica glass structure and have seen that small increases of pressure activate the DWP in different regions of

(tetrahedral) glass network. This suggests that the DWP as envisaged in [8] are evenly spread throughout the glass structure, each with a different potential barrier that can be changed with pressure.

At higher pressures, the motions in the DWP involve changes of the local topology—local regions of the glass network become unstable and relax, giving rise to large atomic displacements. These motions then lead to changes of local topology, including breaking of some of the initial bonds and forming of new ones. We have seen that rebonding events result in the appearance of increased coordination numbers and the formation of small rings of linked polyhedra, leading to densification. A new feature in this work has been the observation of continued rebonding events following the initial period of response to the application of pressure, which further change the topology. These are dynamic events which occur at a fixed volume. We have called these events coordinons, because they lead to the transfer of a coordination state between SiO_x polyhedra. The changes in structure due to the coordinons ultimately lead to irreversible changes on decompression.

We have studied the irreversibility of the topological changes and densification in silica glass by quantifying the degree of rebonding on compression and decompression. We have seen that pressurizing of the glass structure involves breaking of a considerable proportion of original bonds which are not reformed on the release of pressure. At the same time, a similar number of new bonds are formed under pressure. The stability of the portion with newly acquired bonds leads to the densification of the glass on pressure removal.

Evolving pressurized glass structures in MD simulation we have seen that its volume decreases, consistently with the experimental observations [9]. This has been accompanied by rebonding events that led to the appearance of more closely packed structure and densification. This has enabled us to suggest that rebonding processes observed in this work are related to the continuous relaxation observed experimentally in pressurized silica glass [9]. We have seen that higher temperature increases the degree of rebonding, promoting the densification of the decompressed structure.

Acknowledgment

We are grateful to the EPSRC (UK) for support.

References

[1] Williams Q and Jeanloz R 1998 *Science* **239** 902
Grimsditch M 1984 *Phys. Rev. Lett.* **52** 2379
Polian A and Grimsditch M 1990 *Phys. Rev.* B **41** 6086
Hemley R J, Mao H K, Bell P M and Mysen B O 1986 *Phys. Rev. Lett.* **57** 747
Mackenzie J D 1963 *J. Am. Ceram. Soc.* **46** 461
Meade C, Hemley R J and Mao H K 1992 *Phys. Rev. Lett.* **69** 1387
[2] Susman S, Volin K J, Price D L, Grimsditch M, Rino J P, Kalia R K, Vashishta P, Gwanmesia G and Liebermann R C 1991 *Phys. Rev.* B **43** 1194
[3] Jin W, Kalia R K, Vashishta P and Rino J P 1993 *Phys. Rev. Lett.* **71** 3146
Jin W, Kalia R K, Vashishta P and Rino J P 1994 *Phys. Rev.* B **50** 118
Tse J S, Klug D D and Page Y L 1992 *Phys. Rev.* B **46** 5933
[4] Della Valle R G and Venuti E 1996 *Phys. Rev.* B **54** 3809
[5] Trachenko K, Dove M T, Hammonds K, Harris M and Heine V 1998 *Phys. Rev. Lett.* **81** 3431
[6] Trachenko K, Dove M T, Harris M and Heine V 2000 *J. Phys.: Condens. Matter* **12** 8041
[7] Trachenko K, Dove M T and Heine V 2002 *Phys. Rev.* B **65** 092201
[8] Anderson P W, Halperin B I and Varma C M 1972 *Phil. Mag.* **25** 1
Philips W A 1972 *J. Low Temp. Phys.* **7** 351

[9] Tsiok O B, Brazhkin V V, Lyapin A G and Khvostantsev L G 1998 *Phys. Rev. Lett.* **80** 999
[10] Smith W and Forester T 1996 *J. Mol. Graph.* **14** 136
[11] Wooten F, Winer K and Weaire D 1985 *Phys. Rev. Lett.* **54** 1392
Wooten F and Weaire D 1987 *Solid State Physics* vol 40 (New York: Academic) p 1
[12] Tsuneyuki S, Tsukada M, Aoki H and Matsui Y 1988 *Phys. Rev. Lett.* **61** 869
[13] Tsuneyuki S, Matsui Y, Aoki H and Tsukada M 1989 *Nature* **339** 209
[14] Lacks D J 1988 *Phys. Rev. Lett.* **80** 5385
[15] Lacks D J 2000 *Phys. Rev. Lett.* **84** 4629
[16] Trachenko K and Dove M T 2002 *J. Phys.: Condens. Matter* **14** 1143
[17] Zeller R C and Pohl R O 1971 *Phys. Rev.* B **4** 2029
[18] Mukherjee G D, Vaidya S N and Sugandhi V 2001 *Phys. Rev. Lett.* **87** 195501
[19] El'kin F S, Brazhkin V V, Khvostantsev L G, Tsiok O B and Lyapin A G 2002 *JETP Lett.* **75** 342